Supporting Information

Resonance Energy Transfer between Quantum Dots and Diverse Fluorescent Proteins

Igor L. Medintz, Thomas Pons, *et al*.,

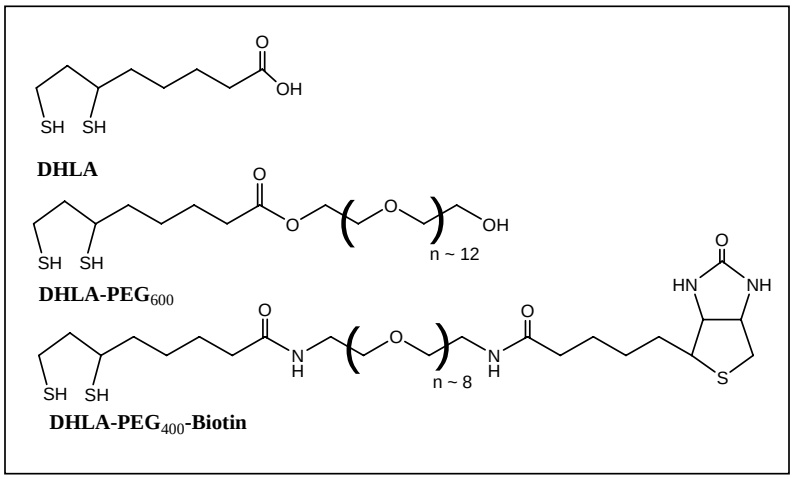

Figure S1. Chemical structures of the ligands used in this study. Dihydrolipoic acid (DHLA), DHLA appended with polyethylene glycol (PEG) segments of MW = 600 (DHLA-PEG_{600}), DHLA appended with biotin-terminated PEG MW = 400 (DHLA-PEG_{400}-biotin); n designates the approximate number of ethylene oxide repeats in the ligand.

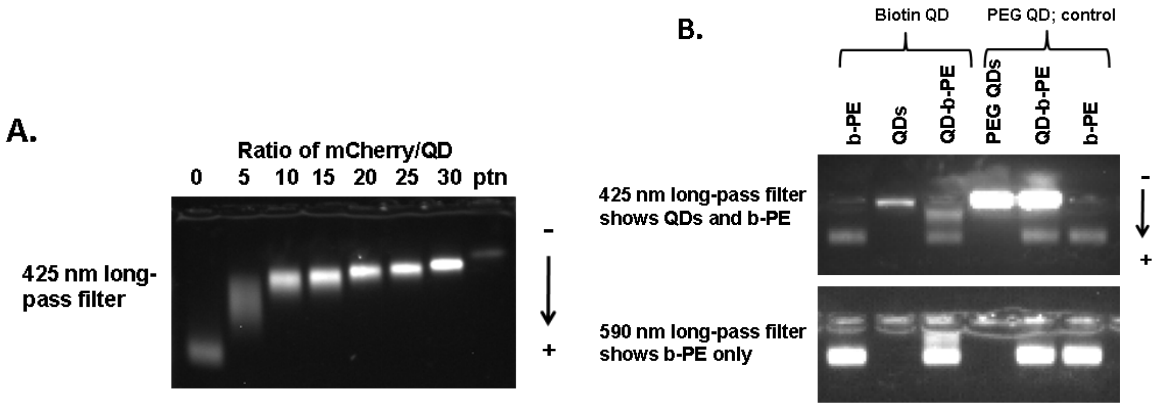

Figure S2. Changes in the gel mobility shift of QDs (emitting at 550 nm) following self-assembly with increasing number of His-appended mCherry **(A)** and QDs (540 nm emission) coupled to Streptavidin-b-PE (**B**). Protein only bands were also shown in column 8 (top) and columns 1&6 (bottom). Similar data were recorded for QD-YFP conjugates. For the Streptavidin-b-PE-QDs a large excess of the protein was added to the QDs during self-assembly to allow visualization of the QD-protein complex and to check for non-specific interactions with DHLA-PEG_{600}-QDs (no biotin). The mobility data were collected using 2% agarose gels.

Self-assembly of an increasing number of mCherry proteins on the QD (capped with DHLA) reduces the QD mobility shift due to a combination of larger size and alteration in the overall charge of the conjugates, as shown in Figure S2A. For the data with b-PE shown in Figure S2B the gel electrophoresis experiments were run using biotin-functionalized QDs (column 1-3) and DHLA-PEG QDs (no biotin, column 4-6). The use of different filters allowed us to either visualize the QD and b-PE fluorescence (425 nm long-pass) simultaneously, or the b-PE emission alone (590 nm long-pass). Data indicate that an intermediary mobility band between the QD and b-PE bands (column 3) representing the QD-b-PE complex appears only for b-PE mixed with biotinylated QDs. The rather small mobility shift measured for the QDs and their conjugates (shown in Figure 2SB) results from the small charges; they both are essentially neutral. Only the individual bands attributed to QDs and proteins appears in the sample made using DHLA-PEG QDs (column 4-6).

Collection of lifetime data. The time-dependent fluorescence measurements were performed using a time-correlated single-photon counting system (Medintz, Clapp *et al.* 2005; Clapp, Pons *et al*. 2007). Briefly, the excitation source consisted of a synchronously pumped dye laser that was pumped by the second harmonic (527 nm) of a Nd:YLF laser operating at 100MHz. The dye laser was equipped with a single plate birefringent filter tuned to produce laser oscillation at 610 nm with a full width at half maximum pulse width of ~1 ps. The dye laser was cavity-dumped at 1 MHz, and then frequency doubled using a potassium dihydrogen phosphate nonlinear crystal to produce the excitation signal (at 305 nm) we used. Sample fluorescence was spectrally filtered with a monochromator (bandpass ~10 nm) and detected with a cooled microchannel plate PMT (Hamamatsu R2809U-11, Shizuoka Japan). Temporal response function of the system was measured to a FWHM of ca. 50 ps.

Analysis of the mCherry acceptor time-resolved fluorescence. Time-resolved fluorescence of acceptors typically shows a bi-exponential behavior with a rise at short time followed by decay at longer times. For a simple dye-to-dye FRET system, assuming the absence of direct acceptor excitation, the sensitized acceptor fluorescence can be described by an expression of the form:

$$I_{acc}(t) = -A\exp(-t/\tau_d) + A\exp(-t/\tau_{acc}), \qquad \text{(S1)}$$

where τ_d and τ_{acc} are the donor and acceptor lifetimes. The weighting constant A can be either positive or negative, depending on which decay time (τ_d or τ_{acc}) is faster. The rise is always associated with the fastest decay time (Lakowicz 2006).

For QD donors the system is complicated by the fact that the donor exciton decay is best described using a multi-exponential form, due to population heterogeneity and fluctuations of non-radiative rates. We took this multi-exponential behavior into account and fitted the time-resolved fluorescence signal of the acceptor using an expression of the form:

$$I_{acc}(t) = -A_r \exp(-t/\tau_r) + A_1 \exp(-t/\tau_1) + A_2 \exp(-t/\tau_2) + A_3 \exp(-t/\tau_3), \quad \text{(S2)}$$

where the first term account for the fast intensity rise of the acceptor signal (occurring at very short time following the excitation pulse) and the others describe the slower multi-exponential decay. Fitting the data shown in Figure 3B to Equation S2 provided values for the rise time, $\tau_{r,}$ and an average amplitude weighted decay time, τ_{Av} for each conjugate valence (using Equation 1, see Table II). Attributing the dynamics observed in the rise and decay times to specific photophysical parameters is not as straightforward as in a standard dye-to-dye FRET pair. Indeed the lifetimes shown in Table II are average (using Equation 1) of two decay rates, one is close that of the mCherry (~1 ns), while two other fractions of the QD population exhibited slower decay rates (~2-3 ns or ~8-10 ns) (data not shown). We should emphasize, however, that the QD decay and mCherry rise versus conjugate valence follow the same trend: both are accelerated at higher mCherry-to-QD ratios. This is an indication that they both originate from the same FRET channel (between QD and mCherry), which increases with the QD-mCherry valence. Further, more sophisticated and quantitative analysis of the mCherry dynamics is hampered by the heterogeneity of the QD photodynamics.

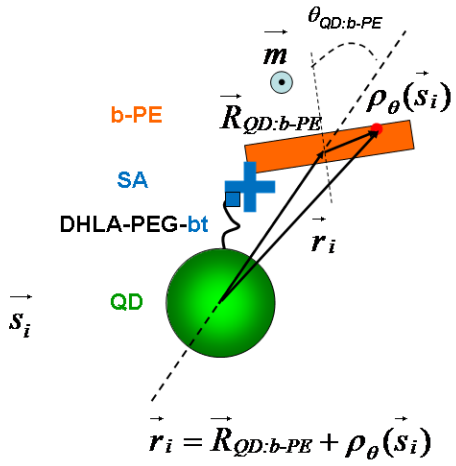

Figure S3. Schematics of the QD-b-PE conjugates showing the geometrical definition of the distance r_i form the QD canter to individual chromophore *i.*

Analysis of the quenching efficiency of a QD donor by a single b-PE acceptor (due to FRET) must take into account the discrete positions of the individual chromophores in the protein, rather than simply abstracting the full protein to a monomeric acceptor. The position of each chromophore with respect to the QD can be described by two parameters: center-to-center QD:b-PE separation distance, $R_{QD:b\text{-}PE}$, and the angle between a b-PE axis ($\vec{m}$) and the QD:b-PE center-to-center axis, $\theta_{QD:b\text{-}PE.}$ We define $\vec{s}_i$ the vector between the b-PE center and the position of chromophore i, as described in the crystallographic structure 1B8D. We set $\rho_\theta(\vec{s}_i)$ the image of $\vec{s}_i$ by the rotation around $\vec{m}$ with the angle $\theta_{QD:b\text{-}PE}$. $\rho_\theta(\vec{s}_i)$ (see Figure S3). The vector $\vec{r}_i$ between the QD center and the individual chromophore *i* can then be geometrically described as the sum of the QD center-to-b-PE center vector, $\vec{R}_{QD:b\text{-}PE}$, and $\rho_\theta(\vec{s}_i)$:

$$\vec{r}_i = \vec{R}_{QD:b\text{-}PE} + \rho_\theta(\vec{s}_i)\,. \qquad \text{(S3)}$$

References:

A. R. Clapp, T. Pons, I. L. Medintz, J. B. Delehanty, J. S. Melinger, T. Tiefenbrunn, P. E. Dawson, B. R. Fisher, B. O'Rourke and H. Mattoussi, "Two-photon excitation of quantum dot-based fluorescence resonance energy transfer and its applications." *Adv. Mater.*, 2007, 19, 1921-1926.

Lakowicz, J. R. (2006), *Principles of Fluorescence Spectroscopy*, Springer, New York.

I. L. Medintz, A. R. Clapp, J. S. Melinger, J. R. Deschamps and H. Mattoussi. "A reagentless biosensing assembly based on quantum dot donor Förster resonance energy transfer." *Adv. Mater.*, 2005, 17, 2450-2455.